ICES C.M. 1996/S:6
The Shelf Edge Current
and its Effects on Fish Stocks

Eddy-Induced Flow of Scotian Shelf Water Across Northeast Channel, Gulf of Maine

J. J. Bisagni
National Oceanic and Atmospheric Administration
National Marine Fisheries Service
Narragansett, Rhode Island, 02882, USA
bisagni@fish1.gso.uri.edu

P. C. Smith
Department of Fisheries and Oceans
Bedford Institute of Oceanography
Dartmouth, Nova Scotia, B2Y4A2, Canada
pc_smith@bionet.bio.dfo.ca

ABSTRACT

Historical and recent data show the episodic occurrence of cold, low salinity water, flowing southwestward along the outer shelf on southern Georges Bank during spring. Careful analysis indicates that the southwestern Scotian Shelf is the source of this water. For example, during April-June 1995, sea surface temperature (SST) images derived from infrared satellite data show intermittent, curvilinear tongues of cold Scotian Shelf Water (SSW) crossing Northeast Channel from Browns Bank to eastern Georges Bank. During one particular event (23 April-1 May 1995), SST patterns were found to be consistent with cross-channel flow of SSW along the northern margin of a cyclonic eddy located within Northeast Channel. In addition, SST patterns during the period suggest that the cyclonic eddy is elliptical, with a greater along-channel dimension (~50 km) relative to its cross-channel dimension (~25 km). Furthermore, subsurface temperature, salinity and velocity from mooring NECE (42° 18' N, 65° 51' W) located in Northeast Channel show evidence for the passage of a cyclonic eddy through the mooring array during the same time period. The cyclonic eddy's influence at NECE was noted throughout the entire water column. The strength and frequency of such eddies in Northeast Channel may play a large role in controlling the injection of mass, heat, salt, plankton and small fish onto Georges Bank during spring.

INTRODUCTION

Based on oxygen isotope data, the mean flow along the Scotian Shelf and the southern New England Shelf is continuous and equatorward due to buoyancy-driven currents forced by glacial melt and river runoff from southern Greenland, Hudson Strait and coastal Labrador (Fairbanks, 1982; Chapman *et al.*, 1986; Chapman and Beardsley 1989). However, strong bathymetric features such as Northeast Channel, Georges Bank and Great South Channel separate the Scotian Shelf from the Southern New England Shelf (Fig. 1). Therefore, dynamically-constrained Scotian Shelf flows enter the Gulf of Maine by turning clockwise, following the local bathymetry south of Cape Sable (Smith, 1983; Smith, 1989a; Smith, 1989b) and on the northeastern side of Northeast Channel (Ramp *et al.*, 1985). Flow within the Gulf of Maine is generally cyclonic (Bigelow, 1927) due to the buoyant coastal current formed from the inflowing Scotian Shelf water (SSW), local river runoff and cyclonic gyres over Georges and Jordan Basins resulting from deep inflows of slope water (Brooks, 1985; Brooks and Townsend, 1989; Brown and Irish, 1992; Bisagni *et al.*, 1996) and possibly warm-core Gulf Stream ring water through Northeast Channel (Brooks, 1987). However, large amounts of freshwater within the Gulf can sometimes result in anticyclonic flow over Jordan Basin (Brown and Irish, 1992). Wintertime mixing of low salinity SSW with higher salinity slope water results in Maine intermediate water (Hopkins and Garfield, 1979), which exits the Gulf by flowing around northeastern Georges Bank during spring-summer (Flagg, 1987) together with along-shelf transport onto the southern New England Shelf south of Nantucket (Beardsley *et al.*, 1985) and into Great South Channel (Chen, 1992). Low salinity water exits the western Gulf of Maine and flows onto northern Georges Bank by late spring-summer (Chen, 1992) in addition to replenishment of central Georges Bank water from the western Gulf during fall-winter (Hopkins and Garfield, 1981).

Historical data suggest that SSW may also cross Northeast Channel episodically, despite dynamic constraints, flowing directly onto Georges Bank from the southwest Scotian Shelf during winter-spring, thus reducing the time required to reach eastern Georges Bank, relative to the more circuitous path around the Gulf of Maine. Data collected sporadically between 1912-1987 suggests that of the ten years with adequate spatial coverage (1934, 1940, 1941, 1965, 1966, 1978, 1979, 1982, 1984 and 1985) during a seventy-six year period, water with salinity of less than 32.0 psu was found on southern Georges Bank only during May of 1941, 1966 and 1978, or three out of the ten years (Bisagni *et al.*, in-press). Optimally-interpolated, satellite-derived sea surface temperature (SST) and hydrographic data confirm that the southwest Scotian Shelf is the source of cold, low salinity waters observed on southern Georges Bank during winter-spring 1992 and 1993 in agreement with earlier surveys (Bigelow, 1927; EG&G, 1980; Hopkins and Garfield, 1981; Flagg, 1987) and also show large interannual variability in the transport and/or properties of SSW crossing Northeast Channel onto Georges Bank (Bisagni *et al.*, in-press). A large cross-Channel flow during late winter-spring 1992 shows cold (less than 2.0 °C), low salinity (less than 32.0 psu) SSW extending seaward along southern Georges Bank on 1 March 1992 with the shelf-slope front located ~100-km seaward of the 200-m isobath. Onbank movement of SSW during April 1992 resulted in monthly-averaged near-surface temperatures decreasing to a minimum of approximately 2.5 °C by April 1992 and temperatures greater than one standard deviation below the long-term mean temperature at NOAA buoy 44011 on southern Georges Bank by May 1992 along with minimum salinity values of less than 32.0 psu (Bisagni *et al.*, in-press). A similar mass of SSW was absent during early March 1993, when cold SSW extended only onto northeast Georges Bank (Bisagni *et al.*., in-press). While lower (higher) salinities measured during spring 1992 (1993) are consistent with higher (lower) St. Lawrence River discharge during spring 1991 (1992) and the ~9-month lag between maximum discharge and minimum salinity near Cape Sable, comparisons between the occurrence of low salinity SSW on southern Georges Bank during May 1966, 1971 and 1978 and lagged St. Lawrence discharge show no similar relationship. Smith (1989b) reached the same conclusion regarding seasonal salinity anomalies from a 6.5-year time series of moored measurements off Cape Sable.

Possible factors that allow SSW flows to break the strong topographic constraint and cross Northeast Channel onto Georges Bank are currently being investigated. In one study, numerical modeling of the adjustment of a barotropic current near a shelf-break to a sharp bend in shelf topography shows that for parameters within the oceanographic range, the adjustment to the bend is smooth and steady with no eddies being shed at the "corner" (Williams, 1995). Such "smooth" adjustment suggests that other factors such as stratification, wind stress and time-dependent inflows must play a role in the ability of SSW flows to cross Northeast Channel onto Georges Bank (Williams, 1995). In this paper, we present both raw and optimally-interpolated satellite-derived SST data along with moored hydrographic and current meter measurements showing SSW crossing Northeast Channel along the northern margin of an elliptical cyclone which became trapped within Northeast Channel during spring 1995. Although we emphasize the general coherence between the satellite and moored observations of this single feature, only through an understanding of the strength and frequency of such features can their importance to the transfer of mass, heat, salt, plankton and small fish between the Scotian Shelf and Georges Bank be assessed.

METHODS

Satellite-Derived Sea Surface Temperature

Advanced Very High Resolution Radiometer (AVHRR) data were collected from 15 September 1994-30 July 1995 by the NOAA-9 polar-orbiting satellite. Data were preprocessed using the standard split window algorithm of McClain *et al.* (1985) to correct for atmospheric absorption, followed by conversion to sea surface temperature (SST) and earth-located (Cornillon *et al.*, 1987) to the large ~700 x 700-km study region (Fig. 1). This initial processing resulted in a 319-day time series of raw 512 x 512 pixel SST images at a spatial resolution of ~1.4 km. Inspection of all raw SST imagery provided a series of 17 images (2 April-10 May 1995) containing cloud-free SST data which were used to locate the cyclonic feature present within Northeast Channel. The feature's center was digitized from each of the 17 raw SST images and its distance along the axis calculated using the projected location of the NECE mooring along the Channel's axis as the origin.

In order to overcome cloud-induced "gappiness" in the raw data, clouds were eliminated from all raw images by automated (Cayula and Cornillon, 1992) and manual (Bisagni and Sano, 1993) flagging procedures. Optimal interpolation (OI) (Chelton and Schlax, 1991; Bisagni *et al.*, 1996) was then used to produce sixty-four, five-day averaged SST maps at five-day intervals beginning at noon (UT) 24 September 1994 (yearday 267) and ending at noon (UT) 5 August 1995 (yearday 217). OI weights were computed using an analytical function fitted to the raw autocorrelation computed from near-surface (~1-m depth) temperatures at NOAA buoy 44005 located in the central Gulf of Maine (Fig. 1). The initial time lag between an OI estimate and input observations was set to 5 days. The number of observations used to compute an OI estimate was set to 8. Non-seasonal SST signal and noise variances were set to 0.91 $(°C)^2$ and 0.06 $(°C)^2$, respectively, given a root-mean-square uncertainty of 0.75 °C for a single SST retrieval and 10 degrees of freedom. A 1982 Gulf of Maine analysis yielded a root-mean-square difference of 0.72 °C (N=39,322) between "same day" input raw SST observations and output OI SST estimates, with a correlation coefficient of 0.98 ($p \leq 0.05$) (Bisagni *et al.*, 1996). For this study, one-day OI SST maps were produced by linear interpolation from the five-day OI SST maps for yeardays 91-181 (1 April-30 June) 1995 over the ~7-km resolution (66 x 41) mapping grid contained within 65.05–68.95° W, 41.25–43.25° N (Fig. 1). A subset of the one-day OI SST maps is used to assess the correspondence between the SST expression of the Northeast Channel cyclone and sub-surface measurements at mooring NECE.

Subsurface Measurements at Mooring NECE

The NECE mooring is part of a three element array deployed by Dartmouth College and Canada's Department of Fisheries and Oceans. This mooring was deployed on the northeast side of Northeast Channel (Fig. 1) and carried five Aanderaa RCM-8 current meters at nominal depths of 23, 50 100, 150, and 190 m, set to sample current speed and direction, pressure, temperature, and conductivity at 1-hour intervals. The estimated accuracies for the deeper ($\geq$50 m) measurements of Aanderaa speed ($\pm$1.3% at speeds over 0.2 ms^{-1}), direction ($\pm$5°) and temperature ($\pm$0.04°C) were determined from laboratory calibrations; whereas the near-surface speeds and directions are accurate to roughly $\pm$0.01 ms^{-1} and $\pm$10°, respectively (Smith, 1989a). Unfortunately, the conductivity cells on the top three instruments from this mooring (23,50, and 100 m) showed signs of biological fouling on recovery and postcalibrations against nearby CTD profiles indicate offsets of order (-2.20, -0.80, and -0.20) had developed in the salinity records during the early part of 1995. The salinities from deeper instruments (150, 190 m) agreed with the CTD to within $\pm$0.10. Thus, the salinity records at 23 and 50 m will be ignored; those at 100, 150 and 190 m are considered accurate to $\pm$0.30, $\pm$0.10, and $\pm$0.10, respectively. The safety of the mooring from the intense fishing pressure in the area was insured, partly, by placement within a triangular array of three surface guard buoys, consisting of 1.3 m steel spheres with masts carrying both lights and radar reflectors.

Hourly data were low-pass filtered using a 129-point Cartwright filter with a high-frequency cutoff at 0.036 cph, and subsampled at 6-hour intervals. At the same time, currents were resolved into cross-channel (+u towards 42°T) and along-channel (+v towards 312°T) components, in agreement with the coordinate system of Ramp *et al.* (1985). Further filtering to daily mean values was accomplished by applying a five-point running mean. Anomaly time series were created by subtracting a 60-day (yearday 81-140) mean from the hourly records prior to filtering to focus on the particular period of interest. These residual data were particularly useful in describing the current fluctuations associated with observed mesoscale features.

Wind Response Estimation

Ramp *et al.* (1985) demonstrated a coherent relationship between Gulf-wide barotropic pressure gradients, detected by synthetic subsurface pressure (SSP) measurements at Portland, Maine, and deep (150 m) along-channel currents in Northeast Channel for periods of 2-22 days (except near 3.75 d). They have also shown that SSP at Portland, Maine, is coherent with cross-(along-) channel wind stress components for periods of 5.6-22 (5.6 only) days. As a result of these relationships, an Ekman-induced, wind-forced "setup" model was proposed for deep currents within Northeast Channel (Ramp *et al.*, 1985). Here we adopt a more direct and quantitative approach of frequency-dependent multiple regression analysis (e.g. Drinkwater, 1994), by which the current components, u and v, are modeled as linear functions of the cross- and along-channel wind stress components, τ^x, τ^y, as:

$$Y_i = H_{ix}\tau^x + H_{iy}\tau^y + Z_i \qquad (1)$$

where Y_i is the velocity component at frequency i, H_{ix} and H_{iy} are the frequency-dependent response functions, and Z_i is residual noise. The response functions are defined by,

$$H_{ix} = G_{ix}e^{iF_{ix}}, \quad H_{iy} = G_{iy}e^{iF_{iy}}, \qquad (2)$$

where G_{ix}, G_{iy} are the gains and F_{ix}, F_{iy} are the phase lags of the responses with respect to the forcing. The squared multiple coherence between output and inputs is a measure of the variance explained by the regression.

For a sinusoidal, rectilinear wind stress variation of amplitude, τ_i ,oriented at an angle θ to the y- (along-channel) axis, the amplitude of the response is,

$$|Y_i| = G_i\tau_i, \tag{3}$$

where

$$G_i^2 = (G_{ix}\sin\theta)^2 + (G_{iy}\cos\theta)^2 + 2G_{ix}G_{iy}\sin\theta\cos\theta\cos(F_{ix}-F_{iy}) \tag{4}$$

and the phase angle between Y_i and τ_i is,

$$F_i = \arctan\left[\frac{G_{ix}\sin\theta\sin F_{ix} + G_{iy}\cos\theta\sin F_{iy}}{G_{ix}\sin\theta\cos F_{ix} + G_{iy}\cos\theta\cos F_{iy}}\right] \tag{5}$$

Thus the time dependent response is of the form,

$$Y_i = |Y_i|\cos(\omega_i t + F_i), \tag{6}$$

where ω_i is the frequency. Also the wind stress direction, θ_m , which maximizes the response, $|Y_i|$, is given by (Garrett and Toulany, 1982):

$$\theta_m = 0.5 \arctan\left[\frac{2G_{ix}G_{iy}\cos(F_{ix}-F_{ix})}{G_{iy}^2 - G_{ix}^2}\right]. \tag{7}$$

The wind stress components used for this analysis are the daily-average estimates, derived using the method of Large and Pond (1981) from Fleet Numerical Oceanography Center (FNOC) model winds (adjusted for surface friction; Bakun, 1975) at 42°N, 66°W on Georges Bank. The response functions and other parameters are then computed for cross- and along-channel currents with respect to wind stress components with the same orientations over the period from 22 March (yearday 81) to 20 May (yearday 140), 1995. The cross-spectral analysis is performed with fourteen, 50% overlapping blocks, yielding 23 degrees of freedom (Garrett and Toulany, 1982). Gains are considered significantly nonzero at the 95% confidence level.

RESULTS

Sea Surface Temperature and Currents

Four SST images from the raw 17-image series show a cyclonic feature located initially at the seaward end of Northeast Channel (2 April) and subsequent shoreward movement of the feature (19 April and 5, 10 May) through the Channel, between the southwestern Scotian Shelf and Georges Bank (Fig. 2). Offshore conditions at the time of the cyclone's formation are shown in the 2 April SST image and include a warm-core Gulf Stream ring located southeast of Northeast Channel, with the shelf-slope front located up to ~60-km seaward of the 200-m isobath along the southwestern Scotian Shelf and eastern Georges Bank (Fig. 2). SST patterns associated with the cyclone in all four images show a ~5-10-km diameter region of warmer water which is partly or wholly surrounded by a streamer of colder SSW located along the cyclone's northern and western margins. The SSW streamer extends across Northeast Channel and onto Georges Bank from a large pool of colder SSW located on the southwestern Scotian Shelf (Fig. 2).

The digitized along-axis locations of the cyclone (Fig. 3) and its distance-time history within Northeast Channel (Fig. 4) show an initial period of slow shoreward motion at ~5 cm s^{-1} (yeardays 92-102) followed by a period when the cyclone was nearly stationary and located ~20 km seaward of the NECE mooring (yeardays 102-113). The cyclone resumed shoreward motion at somewhat higher speeds of up to ~20 cm s^{-1} (yeardays 113-124), followed by a reversal to seaward motion at ~5-10 cm s^{-1} from its shore-most position on 4 May (yearday 124) to its last known position on 10 May (yearday 130) (Fig. 4). Given the uncertainty in locating the true center of the feature from each SST image and the large data gaps, the cyclone's positions and its motion along the axis of Northeast Channel are only estimates.

Low-pass filtered sub-surface temperature residuals at NECE measured at depths of 23 and 100 m show extended ~18-day (yeardays ~103-120) and ~25-day (yeardays ~95-120) periods of positive anomaly, respectively, followed by a ~5-6-day period of negative anomaly at both depths (Fig. 5). In addition, temperature anomaly at 100-m depth shows a strong correlation with salinity anomaly, exhibiting fluctuations with characteristic periods of 3-9 days (Fig. 5). Low-passed sub-surface velocity anomalies at NECE for depths of 23 and 100 m show a general clockwise rotation of the velocity vectors for yeardays 101-116, with shorter fluctuations of 2-5 days (Fig. 6).

Twelve, 1-day OI SST maps, covering 3 April-7 May (yeardays 93-127) 1995 comprise a regularly-spaced (one map every three days) time series which will be used to describe the correspondence between SST patterns over Northeast Channel, interpolated positions of the Northeast Channel cyclone and daily-averaged residual velocity at NECE from 23-m and 100-m depth corresponding to each map date (Fig. 7). SST patterns from the OI maps suggest cross-Channel flow of cold SSW from the southwestern Scotian Shelf and onto eastern Georges Bank during the entire period, with the SSW crossing point moving shoreward from the seaward end of Northeast Channel and along the Channel's axis (yeardays 94-103) at the leading edge of the slowly advancing cyclone (Fig. 7).

The cyclone's positions determined from the OI SST maps show that shoreward translation of the cyclone and the region of cross-channel SSW flow slowed greatly between yeardays 103-112. Sub-surface velocity anomalies through yearday 110 show ~2-5-day period fluctuations consisting of alternating veering and backing currents (Fig. 6). Similar fluctuations occur for temperature anomaly which are vertically coherent between 23 and 100-m depth along with covarying positive salinity anomaly fluctuations at 100 m (Fig. 5) as the cyclone remained almost stationary (Figs. 3, 4 and 7), wavering just seaward of NECE.

More rapid shoreward movement of the cyclone between yeardays 110-124 (Figs. 3, 4 and 7) resulted in the observed simultaneous clockwise rotation (veering) of residual velocities at 23 and 100 m (Fig. 6) as the cyclone passed NECE about yearday 115, with a change to negative temperature and salinity anomalies by yearday ~120 as the cyclone moved well shoreward of NECE (Fig. 5). Anti-clockwise flow around the cyclone initiated a second region of cross-Channel flow, directed southeastward and towards the northern flank of Georges Bank, at the shoreward end of Northeast Channel by yearday 121 (Fig. 7), while cross-Channel SSW flow became re-established at the seaward end of Northeast Channel. SST patterns during this period show that the cyclone may have been strongly elliptical, with a greater along-channel dimension (~50 km) relative to its cross-channel dimension (~25 km) (Fig. 7). Furthermore, the earlier increase to positive temperature anomaly at 100 m relative to 23 m during this period, suggests that the cyclone may widen with increasing depth (Fig. 5).

Detailed current records from 23-m and 100-m depth between yeardays 121-124 (Fig. 6) show continued veering of residual velocities, suggesting disruption of the flow behind the cyclone and possible passage of an anticyclone through mooring NECE during the period, with residual velocities at 100 m leading those at 23 m by ~1 day (Fig. 6), although no anticyclone is indicated from SST data. Subsequent movement of the cyclone (by yearday 127) reversed direction (Figs. 3,

4 and 7), with the elliptical cyclone moving slowly seaward, back towards NECE, in agreement with the anti-clockwise (backing) of residual 23 and 100-m velocities at NECE (yearday 125-129) (Fig. 6) and positive temperature and salinity anomalies by yeardays 125 (127) at 23 m (100 m) (Fig. 5). The last SST observation of the cyclone was made on yearday 130, after which, its signature was lost, possibly due to vernal warming of the sea surface and/or dissipation of the feature (Figs. 3 and 4).

Wind Response

Wind stress components at 42°N, 66°W for the 60-day period of interest, oriented along (τ^y) and across (τ^x) Northeast Channel, show two periods of strong winds (yeardays 85-97 and yeardays 121-130) bracketing a relatively quiescent period during which the cyclone passed through the Channel (Fig.8). Spectral analysis indicates that most of the wind energy is found in the along-channel component at periods of 4-8 days, whereas the kinetic energy of the near-surface (23 m) currents in these bands is distributed roughly equally between the along- and cross-channel components (not shown). Nevertheless, the gain estimations derived from the multiple regression analysis indicate that the cross-channel component of stress is most effective at driving along-channel currents at a depth of 23 m, with magnitudes of order 0.5 ms^{-1}/Pa for periods of 2.7-8 days (Fig.9).

At 100 m, the energy in the along-channel current component is significantly larger than that in the cross-channel component. Along-channel gains with respect to both components of wind stress are also larger, exceeding 0.8 ms^{-1}/Pa for the response to τ^x at 4-day periods (Fig. 10). This picture is qualitatively true for all NECE current responses below 100 m, except that the significant gains tend to increase with depth and are found over a larger frequency range.

The maximum statistically-significant (95%) wind responses (Table 1) reflect both the amplification of the along-channel current gain with depth and the expanded frequency range. The responses at 4 days increase to over 1.0 ms^{-1}/Pa, and consistently occur for wind directions near 70°T or roughly the "alongshore" direction defined by the shelf edge and coastlines. Furthermore, phases for these responses are negative, implying that the wind stress fluctuations lead those in the along-channel current. The multiple coherence estimates indicate that 50-80% of the along-channel component variance is "explained" by the regression.

For the cross-channel current component, the gains are reduced and the wind directions for maximum response vary with depth (Table 1). Near the surface (23 m), the cross-channel component is forced most effectively by the along-channel stress component, whereas the deep cross-channel currents are driven by east-northeastward stresses. Again the phases are mostly negative, indicating that the stress leads the current, and up to 75% of the cross-channel current variance is explained by the regression.

DISCUSSION

The Cyclone's Effect on Georges Bank

Earlier studies have shown the importance of slope water inflow through Northeast Channel to water mass formation (Bigelow, 1927; Colton, 1968; Hopkins and Garfield, 1979; Mountain and Jessen, 1987; Brown and Irish, 1993), interior baroclinic circulation (Bigelow, 1927; Brooks, 1985; Ramp *et al.*, 1985; Brooks and Townsend, 1989; Brooks, 1990; Brown and Irish, 1992), nutrient flux (Schlitz and Cohen, 1984; Ramp *et al.*, 1985; Townsend *et al.*, 1987) and physical-biological coupling within the Gulf of Maine (Townsend and Spinrad, 1986; Townsend *et al.*, 1987; Bisagni *et al.*, 1996). The seasonal cycle of slope water inflow through

Northeast Channel, and its pulse-like variability in the 4-10-day band due to setup of barotropic pressure gradients across the Gulf of Maine by wind stress have also been described (Ramp *et al.* 1985).

We speculate that pulse-like slope water inflows through Northeast Channel may be the source of the discrete slope water cyclones observed previously within Georges and Jordan Basins in the Gulf of Maine (Brooks, 1985; Brooks and Townsend, 1989; Brown and Irish, 1992; Pettigrew and Hetland, 1995). We believe that our limited set of satellite-derived SST and hydrographic measurements were able to observe a single pulse-like inflow of slope water and the resulting slope water cyclone which moved unsteadily within Northeast Channel during April-May 1995. While the SST and subsurface signatures of the cyclone eventually disappeared due to vernal warming or dissipation of the feature, the importance of the cyclone's effect in directing SSW flows across Northeast Channel from the southwestern Scotian Shelf to Georges Bank during the observation period is clearly established, in agreement with the earliest picture of the non-tidal circulation in the region, derived from all available data, which suggests that such a path exists (Bigelow, 1927).

Wind-Forced Translation of the Cyclone

Based upon the wind-forced setup model of Ramp *et al.* (1985), we investigated the relationships between FNOC model estimates of wind stress at 42°N, 66°W, measured currents at 23 and 100-m depth from NECE and translation of the spring 1995 Northeast Channel cyclone. Results which are consistent with the wind setup hypothesis proposed by Ramp *et al.* (1985) show that during spring 1995:

1) "alongshore" wind stress (~70°T) was most effective in producing along-channel flow within Northeast Channel, and

2) phase lags of the maximum current responses behind the wind at 23 and 100-m depth are of order 12-14 hours, in agreement with the inertial time scales required to set up the barotropic pressure gradients.

However, given the relationships listed above, a preliminary assessment of the movement of the spring 1995 cyclone in response to simple advection by wind-driven along-channel flows yields results which are inconclusive. For instance, acting alone, the strong 4-day fluctuation in the cross-channel stress between yeardays 121-129 would induce a 0.07 ms^{-1} maximum along-channel current and a 25 km oscillatory displacement at 23 m at NECE, based on a stress amplitude of 0.14 Pa and an along-channel gain of 0.5 ms^{-1}/Pa. At the 100 m or 150 m levels, the currents and displacements should be nearly twice that large. Such displacements and rates are evident in the trajectory of cyclone positions (Fig. 4), thus supporting the simple advection hypothesis, although the "gappy" temporal resolution does not permit absolute identification of short term oscillations, except perhaps near yearday 124. However, contrary to the simple advection hypothesis, wind stress is quiescent for the period during which the cyclone moved rapidly past mooring NECE (near yearday 115) at a speed of ~20 cm s^{-1} (Fig. 4), a period when wind-forced currents should be minimal. Therefore, pending further detailed study, it appears that the translation mechanism for the cyclone is not simple wind-driven advection. We speculate that other factors within the Gulf of Maine such as local river runoff may affect coastal SSP and cross-Gulf pressure gradients. Future work may be able to address this issue through a direct analysis of SSP from Portland, Maine, and bottom pressure measurements from NECE made during spring 1995.

SUMMARY & CONCLUSIONS

Surface and sub-surface measurements indicate that a single cyclone (or possibly a cyclone-anticyclone pair) moved into Northeast Channel during early April. This feature was long-lived and remained trapped within the Channel during April-early May and may have been the cause of a series of Scotian Shelf water flows which were able to break the dynamical constraints imposed by the local bathymetry and cross Northeast Channel from the southwestern Scotian Shelf and flow onto eastern Georges Bank. An analysis of wind-driven currents at a mooring (NECE) located on the eastern (inflow) side of Northeast Channel is consistent with earlier studies that suggest large-scale barotropic pressure gradients, established by alongshore-directed (~70°T) wind stress, are the primary forcing mechanism for subtidal current fluctuations at periods of 4-8 days. While some of the cyclone's movements are suggestive of simple wind-driven advection, wind-driven advection is clearly not the sole mechanism responsible for the cyclone's movements through Northeast Channel during spring 1995.

ACKNOWLEDGMENTS

The authors would like to thank K. Seemann, NOAA/NMFS and M. MacNeil, DFO/BIO for their diligent work regarding the processing of the satellite and hydrographic data. Special thanks to R. Evans, O. Brown and the remote sensing staff at the University of Miami for providing satellite data and analysis software. This work is being supported with funding provided under the NSF/NOAA US-GLOBEC Northwest Atlantic Georges Bank Program and the Gulf of Maine Regional Marine Research Program.

REFERENCES

Bakun A. (1975) Daily and weekly upwelling indices, west coast of North America, 1967-1973. *NOAA Technical Report* NMFS SSRF-693, NOAA/NMFS, Seattle, WA, 114 pp.

Beardsley R. C., D. C. Chapman, K. H. Brink, S. R. Ramp and R. Schlitz (1985) The Nantucket Shoals flux experiment (NSFE79). Part I: A basic description of the current and temperature variability. *Journal of Physical Oceanography*, 15:713-748.

Bigelow H.B. (1927) Physical oceanography of the Gulf of Maine. *Bulletin of the United States Bureau of Fisheries*, 40:511-1027Chapman, D. C., J. A. Barth, R. C. Beardsley and R. G. Fairbanks (1986) On the continuity of mean flow between the Scotian Shelf and the Middle Atlantic Bight.

Bisagni J. J. and M. H. Sano (1993) Satellite observations of short time scale sea surface temperature variability on southern Georges Bank. *Continental Shelf Research*, 13:1045-1064

Bisagni J. J., D. J. Gifford and C. M. Ruhsam (1996) The spatial and temporal distribution of the Maine Coastal Current during 1982. *Continental Shelf Research*, 16:1-24.

Bisagni J. J., R. C. Beardsley, C. M. Ruhsam, J. P. Manning and W. Williams (in press) Historical and recent evidence concerning the presence of Scotian Shelf water on southern Georges Bank. *Deep-Sea Research*..

Brooks D. A. (1985) Vernal circulation in the Gulf of Maine. *Journal of Geophyiscal Research*, 90:4687-4705.

Brooks D. A. (1987) The influence of warm-core rings on slope water entering the Gulf of Maine. *Journal of Geophyiscal Research*, 92:8183-8196.

Brooks D. A. (1990) Currents at Lindenkohl Sill in the southern Gulf of Maine. *Journal of Geophyiscal Research*, 95:22173-22192.

Brooks D. A. and D. W. Townsend (1989) Variability of the coastal current and nutrient pathways in the eastern Gulf of Maine. *Journal of Marine Research*, 47:303-321.

Brown W. S. and J. D. Irish (1992) The annual evolution of geostrophic flow in the Gulf of Maine: 1986-1987. *Journal of Physical Oceanography*, 22:445-473.

Brown W. S. and J. D. Irish (1993) The annual variation of water mass structure in the Gulf of Maine: 1986-1987. *Journal of Marine Research*, 51:53-107.

Cayula J.-F. and P. Cornillon (1992) Edge detection algorithm for SST images. *Journal of Atmospheric and Oceanic Technology*, 9:67-80.

Chapman D. C., J. A. Barth, R. C. Beardsley and R. G. Fairbanks (1986) On the continuity of mean flow between the Scotian Shelf and the Middle Atlantic Bight. *Journal of Physical Oceanography*, 16:758-772.

Chapman D. C. and R. C. Beardsley (1989) On the origin of shelf water in the Middle Atlantic Bight. *Journal of Physical Oceanography*, 19:384-391.

Chelton D. B and M. G. Schlax (1991) Estimation of time averages from irregularly spaced observations: With application to Coastal Zone Color Scanner estimates of chlorophyll concentration. *Journal of Geophysical Research*, 96:14669-14692.

Chen C. (1992) Variability of currents in Great South Channel and over Georges Bank: Observation and modelling. Ph.D. Thesis, MIT/WHOI Joint Program in Oceanography, Massachusetts Institute of Technology, Cambridge, MA.

Colton J. B., R. R. Marak, S. Nickerson and R. F. Stoddard (1968) Physical, chemical and biological observations on the continental shelf, Nova Scotia to Long Island, 1964-1966. *United States Fisheries and Wildlife Service Data Report* 23, 190 pp.

Cornillon P., C. Gilman, L. Stramma, O. Brown, R. Evans and J. Brown (1987) Processing and analysis of large volumes of satellite-derived thermal infrared data. *Journal of Geophysical Research*, 92:12993-13002.

Drinkwater K.F. (1994) The response of an open stratified bay to wind forcing. *Atmosphere-Ocean*, 32(4):757-781.

EG&G (1980) Thirteenth quarterly report. Appendix F. Analysis report. Prepared for the New York OCS Office, Bureau of Land Management, by EG&G Environmental Consultants, Waltham, Massachusetts, 194 pp.

Fairbanks R. G. (1982) The origin of continental shelf and slope water in the New York bigt and Gulf of Maine: Evidence from $H_2{}^{18}O/H_2{}^{16}O$ ratio measurements. *Journal of Geophysical Research*, 87:5796-5808.

Flagg C. N. (1987) Hydrographic structure and variability. In: *Georges Bank*, R. H. Backus, editor, MIT Press, Cambridge, MA, p. 108-124.

Garrett C. and B. Toulany (1982) Sea level variatiability due to meteorological forcing in the northeast Gulf of St. Lawrence. *Journal of Geophysical Research*, 87:1968-1978.

Hopkins T. S. and N. Garfield III (1979) Gulf of Maine intermediate water. *Journal of Marine Research*, 37:103-139.

Hopkins T. S. and N. Garfield III (1981) Physical origins of Georges Bank water. *Journal of Marine Research*, 39:465-500.

Large W. G. and S. Pond (1981) Open ocean momentum flux measurements in moderate to strong winds. *Journal of Physical Oceanography*, 11:324-336.

McClain E. P., W. G. Pichel and C. C. Walton (1985) Comparative performance of AVHRR-based multichannel sea surface temperatures. *Journal of Geophysical Research*, 90:11587-11601.

Mountain D. G. and P. F. Jessen (1987) Bottom waters of the Gulf of Maine, 1978-1983. *Journal of Marine Research*, 45:319-345.

Pettigrew N. R. and R. D. Hetland (1995) The cyclonic circulation of the eastern Gulf of Maine. The Oceanography Society Fourth Scientific Meeting, April 18-21, 1995, Newport, Rhode Island, (Abstract), p. 73.

Ramp S. R., R. J. Schlitz and W. R. Wright (1985) The deep flow through Northeast Channel, Gulf of Maine. *Journal of Physical Oceanography*, 15:1790-1808.

Schlitz R. J. and E. B. Cohen (1984) A nitrogen budget for the Gulf of Maine and Georges Bank. *Biological Oceanography*, 3:203-222.

Smith P. C. (1983) The mean seasonal circulation off southwest Nova Scotia. *Journal of Physical Oceanography*, 13:1034-1054.

Smith P. C. (1989a) Circulation and dispersion on Browns Bank. *Canadian Journal of Fisheries and Aquatic Sciences*, 46:539-559.

Smith P. C. (1989b) Seasonal and interannual variability of current, temperature and salinity off southwest Nova Scotia. *Canadian Journal of Fisheries and Aquatic Sciences*, 46:4-20.

Townsend D. W. and R. S. Spinrad (1986) Early spring phytoplankton blooms in the Gulf of Maine. *Continental Shelf Research*, 6:515-529.

Townsend D. W., J. P. Christensen, D. K. Stevenson, J. J. Graham and S. B. Chenoweth (1987) The importance of a plume of tidally-mixed water to the biological oceanography of the Gulf of Maine. *Journal of Marine Research*, 45:699-728.

Williams, W. J. (1995) The adjustment of barotropic currents at the shelf break to a sharp bend in the shelf topography. M.S. Thesis, MIT/WHOI Joint Program in Oceanography, Massachusetts Institute of Technology, Cambridge, MA.

TABLE 1

Significant Maximum Wind Responses for
Cross-Channel (u) and Along-Channel (v) Currents at Mooring NECE
(Hyphen indicates insignificant response.)

	Freq. (cpd)	0.000	0.125	0.250	0.375	0.500
Current Component (depth m) Max Gain (ms^{-1}/Pa), Phase (°), Wind Stress Direction (°T), Fract. Var. Explained						
u(23) G_i, F_i, θ_m, r^2		0.385,0 313 0.592	-	0.342,-46 302 0.606	-	-
u(100) G_i, F_i, θ_m, r^2		-	0.331,16 100 0.566	-	-	-
u(150) G_i, F_i, θ_m, r^2		0.373,0 93 0.631	0.457,-3 93 0.752	0.436,-46 74 0.554	0.376,-69 62 0.363	-
v(23) G_i, F_i, θ_m, r^2		-	-	0.520,-61 67 0.526	-	-
v(100) G_i, F_i, θ_m, r^2		-	-	0.981,-33 74 0.705	0.822,-80 77 0.635	-
v(150) G_i, F_i, θ_m, r^2		0.653,0 82 0.521	0.575,-3 103 0.718	1.090,-41 67 0.785	0.919,-63 65 0.592	-

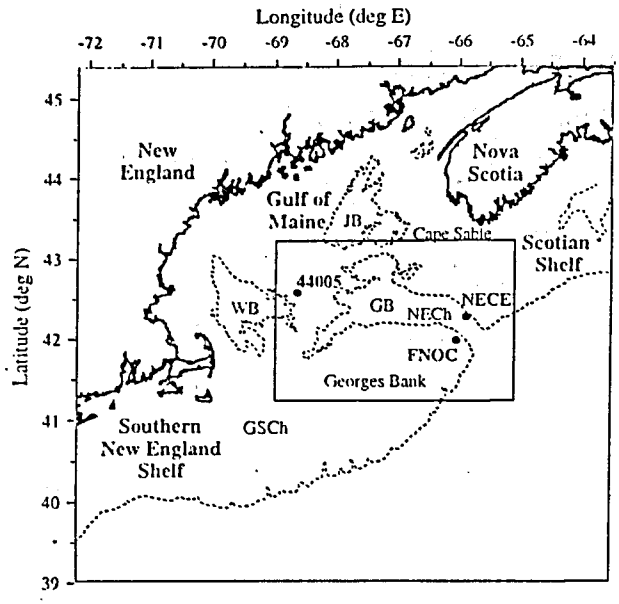

Figure 1. Study area showing the locations of the optimally-interpolated SST mapping grid region (box), the NECE mooring, NOAA data buoy 44005 and the Fleet Numerical Oceanography Center (FNOC) model wind grid point. Also shown are the locations of Georges Basin (GB), Jordan Basin (JB), Wilkinson Basin (WB), Northeast Channel (NECh), Great South Channel (GSCh) and the 200-m isobath (dashed).

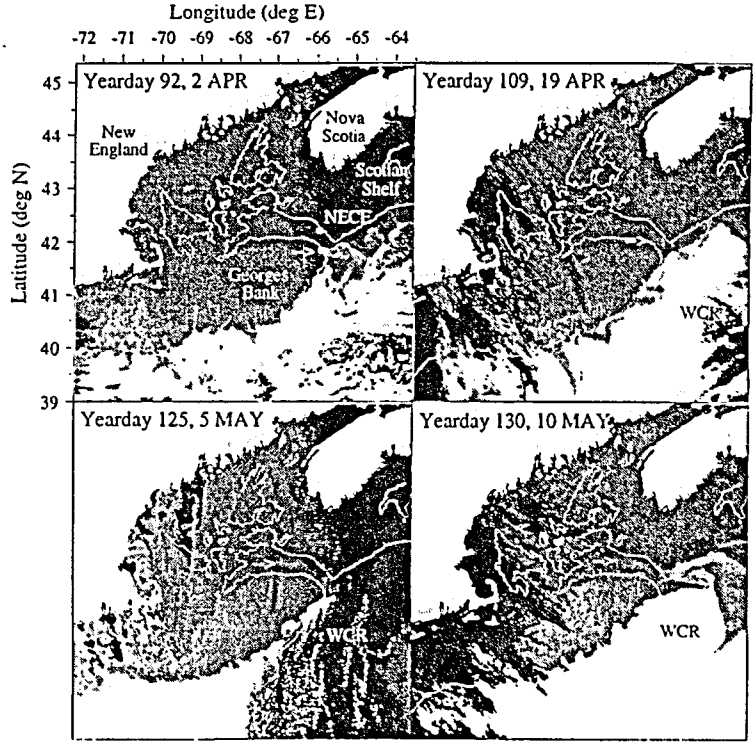

Figure 2. Raw satellite-derived SST images for the study area given in Figure 1 showing the successive locations of the center of a small ~50-km diameter, elliptical, warm-core (~6-7 °C) cyclonic feature (located to the right of the white arrows) which moved into Northeast Channel and past the NECE mooring during April-May 1995. Also shown is the much colder (~3 °C) Scotian Shelf water flowing anti-clockwise around the cyclonic feature, across Northeast Channel and onto eastern Georges Bank, along with a warm-core Gulf Stream ring (WCR) located southeast of Georges Bank by yearday 109 and the 200-m isobath (white line). Warmer (colder) SST values are light (dark). Clouds are black.

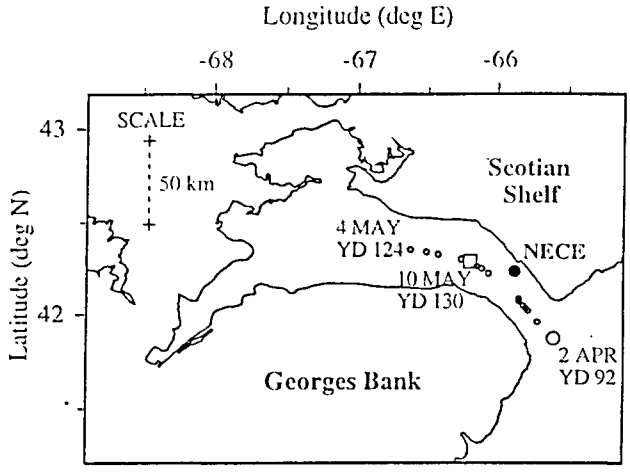

Figure 3. Digitized center positions of the cyclone located within Northeast Channel from 2 April (open circle) -10 May (open square) 1995 as determined from seventeen raw SST images. Also shown is the cyclone's shore-most position on 4 May, the location of the NECE mooring on the northern side of Northeast Channel, a 50-km distance scale (dashed line) and the 200-m isobath (solid line).

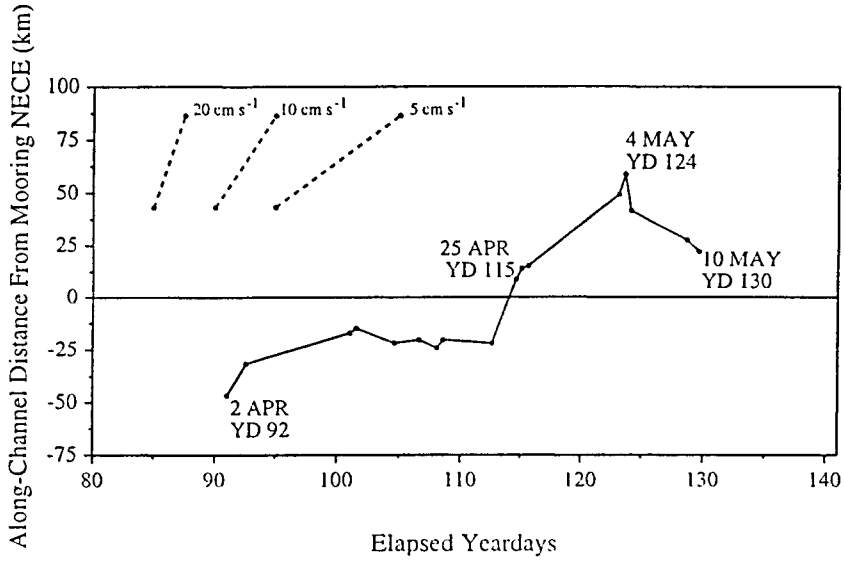

Figure 4. Distance-time history of the digitized center positions of the cyclone located within Northeast Channel from 2 April-10 May 1995 as determined from seventeen raw SST images and shown in Figure 3. Positive (negative) distances are measured in km shoreward (seaward) of the position of mooring NECE projected along the central axis of Northeast Channel. Also shown are three sloped lines (dashed) corresponding to reference speeds of 5, 10 and 20 cm s^{-1}.

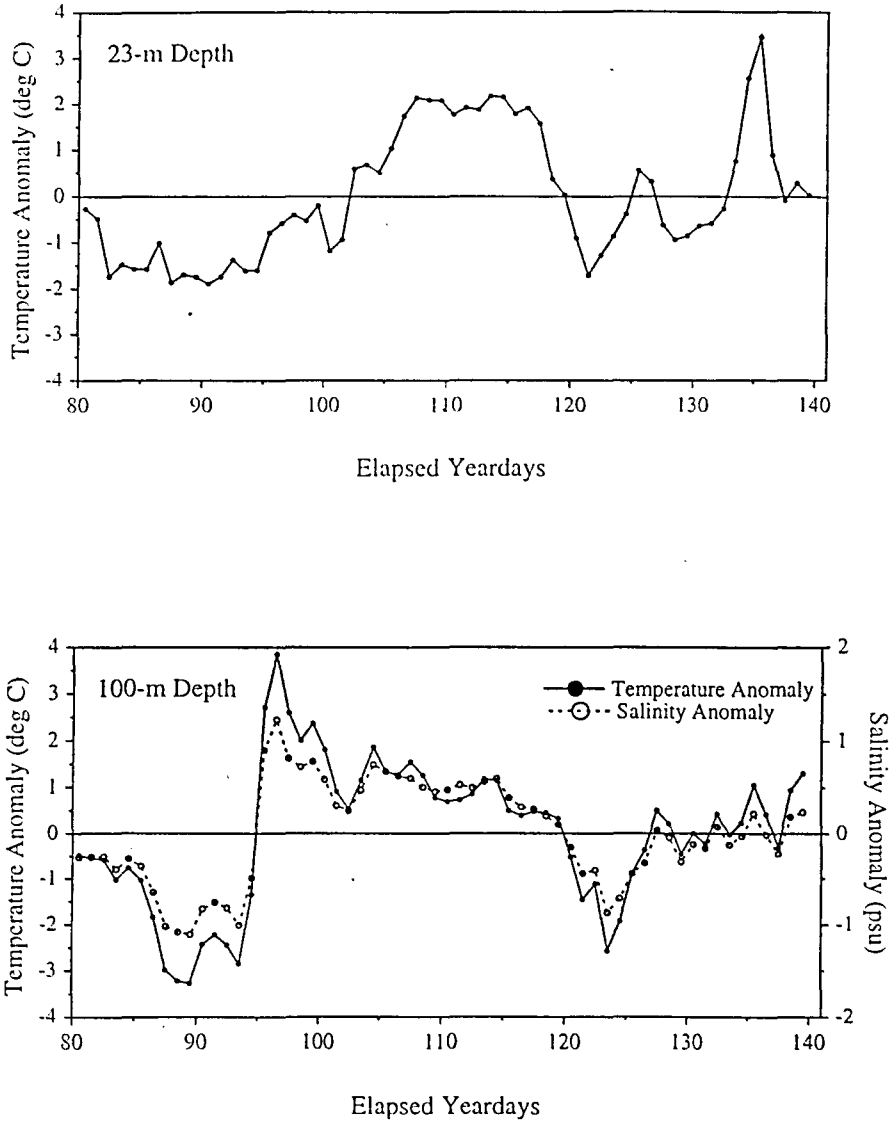

Figure 5. Daily-averaged, low-pass filtered temperature anomaly at 23-m depth at NECE (Top Panel). Daily-averaged, low-pass filtered temperature and salinity anomaly at 100-m depth at NECE (Bottom Panel).

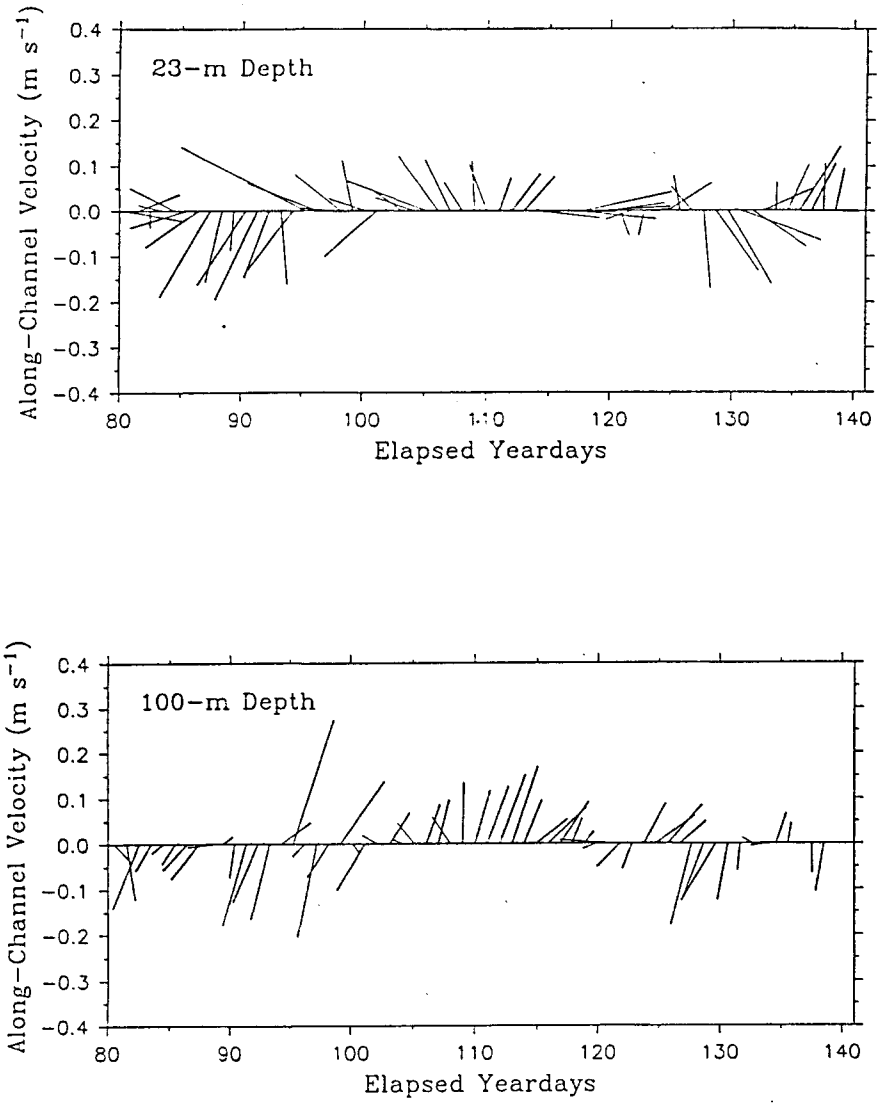

Figure 6. Daily-averaged, low-pass filtered velocity anomaly at 23-m depth at NECE (Top Panel); at 100-m depth at NECE (Bottom Panel).

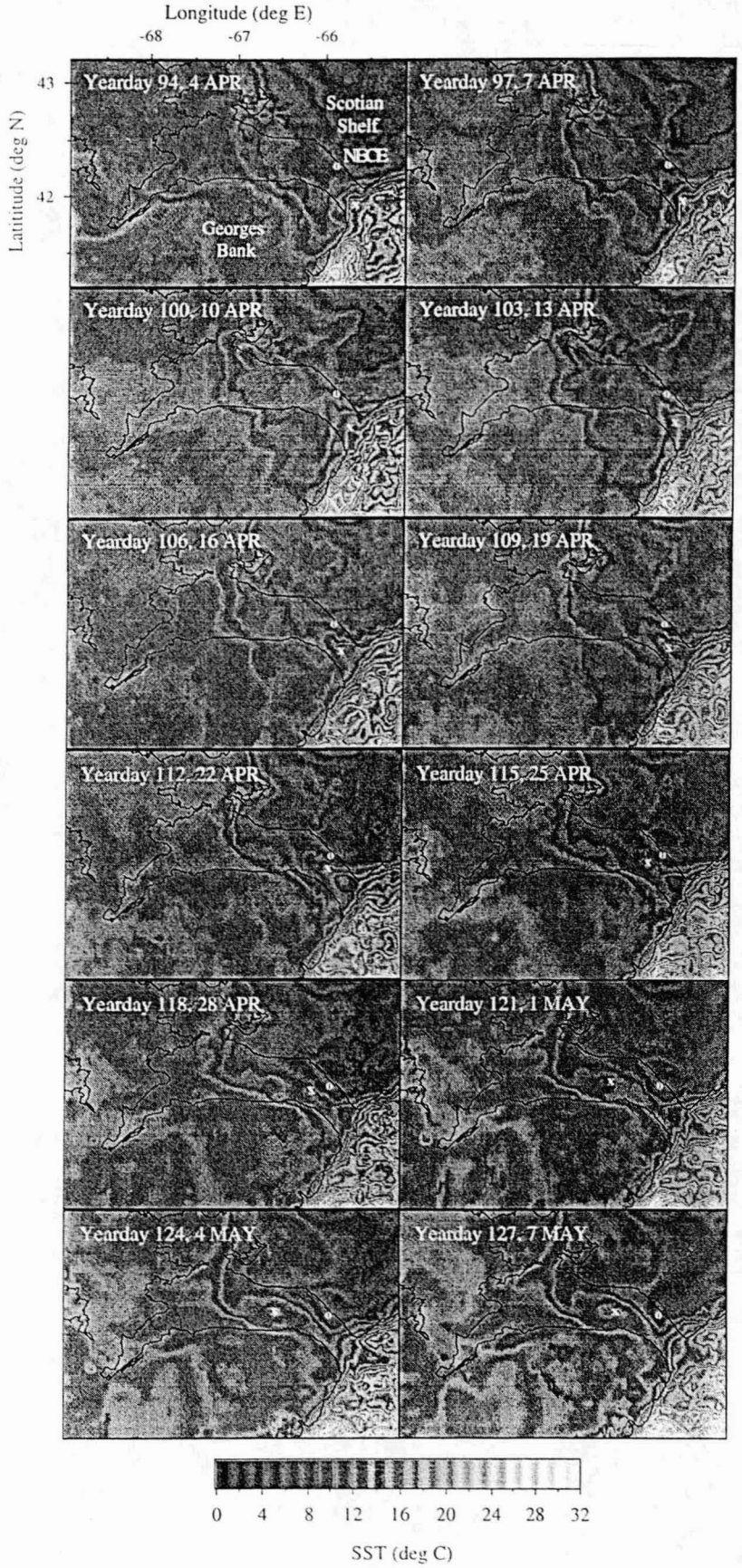

Figure 7. Optimally-interpolated SST maps for the rectangular mapping region shown in Figure 1, showing successive center positions of the cyclone located within Northeast Channel (white "x") from 4 April-7 May 1995, one map every three days. Also shown are the location of the NECE mooring, a SST scale and the 200-m isobath (solid line).

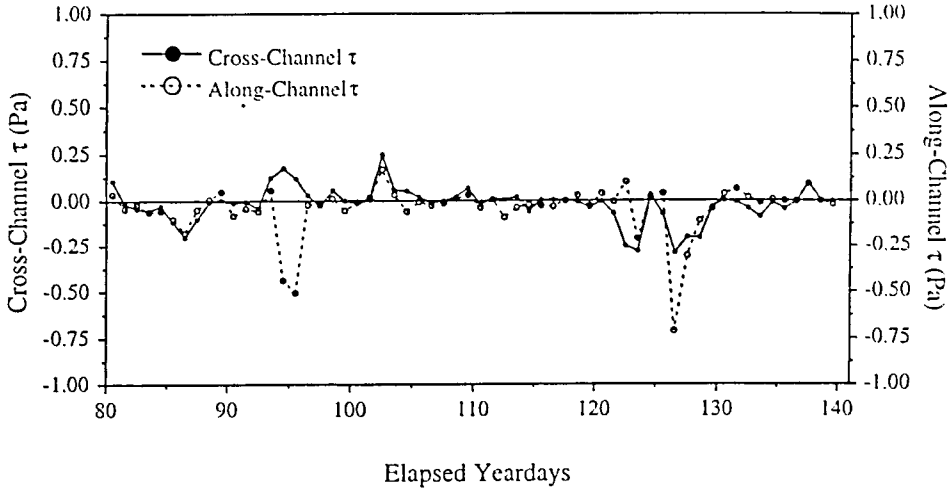

Figure 8. Daily averaged, cross-channel and along-channel wind stress (τ) in Pascals (Pa) computed for the FNOC wind grid point located at 42° N, 66° W on northeastern Georges Bank (see Fig. 1 for location) versus elapsed yearday during 1995. Positive cross-channel (along-channel) stress is directed towards 42° T (312° T).

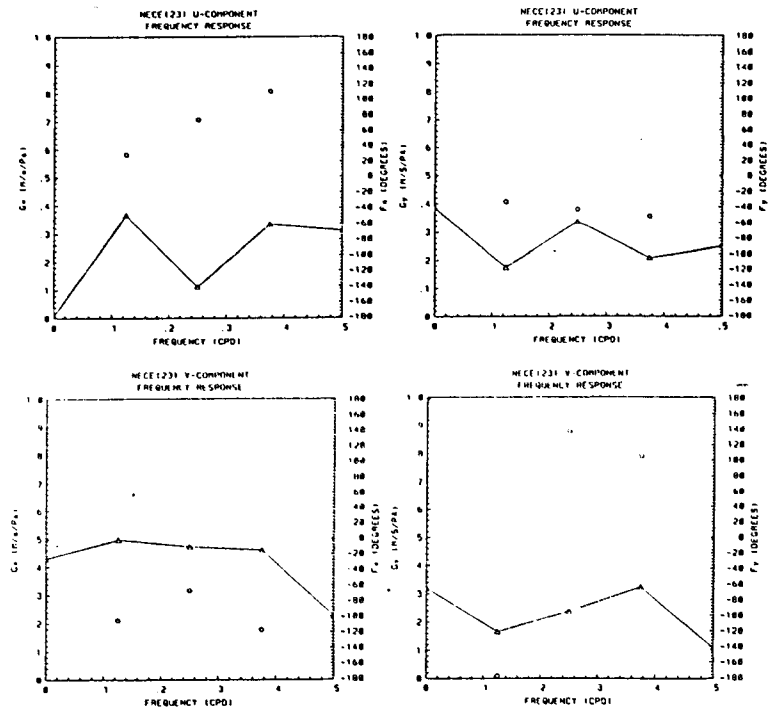

Figure 9. Frequency response functions for along-channel (v) and cross-channel (u) currents with respect to along-channel (τ^y) and cross-channel (τ^x) FNOC wind stress components at 23 m on mooring NECE. Gains (G_x, G_y) and phase lags (F_x, F_y) are represented by open circles and triangles respectively. Negative phase means wind leads current.

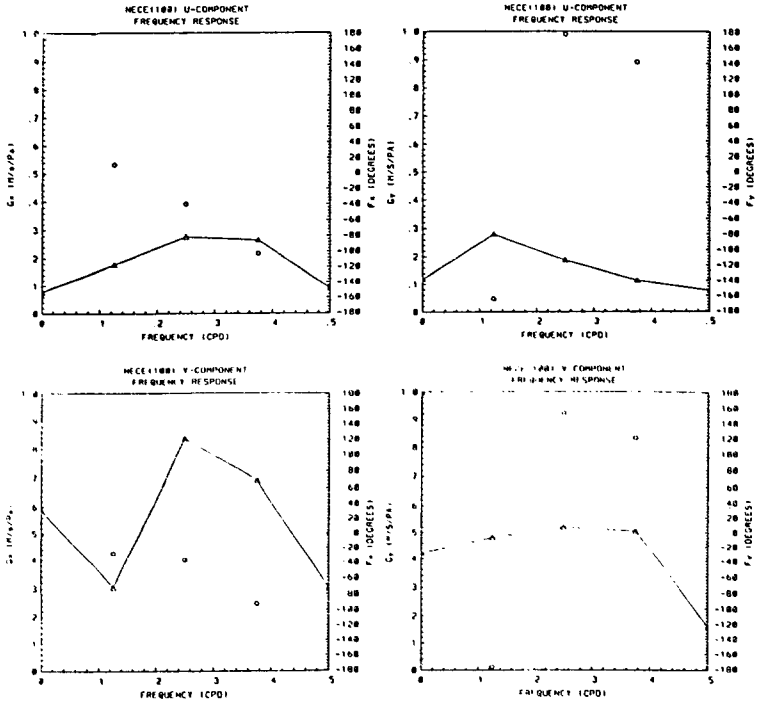

Figure 10. Same as Fig. 9 except for 100-m depth on mooring NECE.